Biodetection using magnetically labeled biomolecules and arrays of spin valve sensors (invited)

H. A. Ferreira, D. L. Graham, P. P. Freitas, and J. M. S. Cabral

Citation: Journal of Applied Physics **93**, 7281 (2003); doi: 10.1063/1.1544449
View online: http://dx.doi.org/10.1063/1.1544449
View Table of Contents: http://scitation.aip.org/content/aip/journal/jap/93/10?ver=pdfcov
Published by the AIP Publishing

Biodetection using magnetically labeled biomolecules and arrays of spin valve sensors (invited)

H. A. Ferreira[a)]
Instituto de Engenharia de Sistemas e Computadores (INESC) and Physics Department, Instituto Superior Técnico (IST), Lisbon, Portugal

D. L. Graham
Instituto de Engenharia de Sistemas e Computadores (INESC) and Centre for Biological and Chemical Engineering, (IST), Lisbon, Portugal

P. P. Freitas
Instituto de Engenharia de Sistemas e Computadores (INESC) and Physics Department, Instituto Superior Técnico (IST), Lisbon, Portugal

J. M. S. Cabral
Centre for Biological and Chemical Engineering, (IST), Lisbon, Portugal

(Presented on 13 November 2002)

On-chip spin-valve sensors ($2\times6\ \mu m^2$) were used to detect the binding of streptavidin-functionalized superparamagnetic labels to sensor surface-bound biotin. Both micron-sized and nanometer-sized labels were studied. The detection of biomolecular recognition was demonstrated using 2 μm Micromer®-M and 250 nm Nanomag®-D labels, with signals ranging from ~300 μV to ~2 mV (8 mA sense current; ~15 Oe in-plane magnetizing fields). For smaller labels, detection of biomolecular recognition was not achieved. The capability of detecting single labels was demonstrated for label moments down to 2×10^{-12} emu (2 μm labels), corresponding to signals of 100–400 μV. Although, theoretical calculations suggest that the minimum measurable moment is in the order of 6×10^{-15} emu, due to noise limitations of the present setup, this limit is in the order of 2×10^{-13} emu, corresponding to a single 250 nm label. On-chip tapered aluminum current line structures were used for placement of magnetic labels at sensor sites. © *2003 American Institute of Physics.* [DOI: 10.1063/1.1544449]

I. INTRODUCTION

The idea of using on-chip magnetic field sensors and magnetic labels for detecting biomolecular recognition, such as the hybridization of two complementary strands of deoxyribonucleic acid (DNA), antibody–antigen interaction or general ligand–receptor binding, dates back to 1996[1] and was first published in 1998.[2] Since then, this area has developed rapidly, generating considerable interest with recent contributions from a number of groups. The first device based on this approach, the Bead Array Counter (BARC) biosensor,[2] incorporated $80\times5\ \mu m^2$ giant magnetoresistance (GMR) sensor strips and used 2.8 μm magnetic labels (Dynabeads® M-280) and has been applied to the detection of biological warfare agents.[3,4] A similar design based on 70 μm diameter GMR spiral sensors has also been proposed recently.[5] In our group, work has been focused on the use of smaller ($2\times6\ \mu m^2$), more sensitive spin-valve sensors, for the detection of single 2 μm (Micromer®-M) microspheres[6] and larger numbers of 400 nm (Nanomag®-D) superparamagnetic particles.[6,7] The same system was then used to detect the binding of streptavidin-functionalized 2 μm labels to sensor-bound biotin.[8] As an alternative to spin-valve and GMR sensors, Hall effect based sensors have also been used recently to detect single 2.8 μm magnetic labels (Dynabeads® M-280).[9]

The immediate advantages of the use of micrometer-sized labels include our demonstrated ability to detect single labels and the visual verification of label position using visible light microscopy. However, the potential disadvantages of using such large label-to-biomolecule size ratio include conformational alterations to the biomolecule and hindrance of biomolecular interaction. In addition, the use of large labels might prevent other labeled biomolecules from interacting with substrate-bound biomolecules in the proximity. This can be avoided in one of two ways: First, use biotinylated target biomolecules to which streptavidin-functionalized microspheres are bound after hybridization (in the case of DNA).[2–5] Alternatively, smaller (nanometer-sized) labels can be used. For these reasons, the use of smaller magnetic labels such as 250 nm (Nanomag®-D), 100 and 50 nm sized particles (Nanomag®-D-spio) has been pursued and will be discussed in this work. A major problem encountered during the use of many nanometer-sized magnetic labels is their tendency to cluster, forming larger magnetic bodies of indiscernible label numbers.

[a)]Author to whom correspondence should be addressed; electronic mail: hferreira@inesc-mn.pt

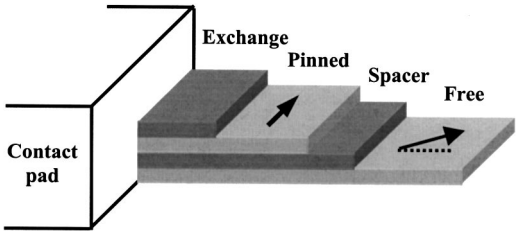

FIG. 1. Schematic of the spin-valve sensor showing the configuration of the magnetic moments in the sense (free) and pinned layers.

II. EXPERIMENTAL METHODS

A. Spin-valve sensors

Spin-valve sensors used have dimensions of $2\times6\ \mu m^2$ (the spin-valve stripe is $14\times2\ \mu m^2$ and the distance between leads is 6 μm). The spin valves were deposited by magnetron sputtering onto 3 in. Si wafers and have the structure Ta 65 Å/NiFe 40 Å/CoFe 10 Å/Cu 26 Å/CoFe 25 Å/MnIr 80 Å/Ta 25 Å/TiW(N) 150 Å. The configuration of the magnetic moments of the sense (free) and pinned layers is shown in Fig. 1. As deposited, the spin-valve coupon sample has a magnetoresistance ratio (MR) of ~7.5% and a square resistance of ~15.4 Ω. The resistance of the $2\times6\ \mu m^2$ sensor is then ~46.2 Ω. Aluminum leads, 1 μm thick are used leading to the wire-bonding pads. After processing, the average MR ratio of the sensor element is $(5.5\pm0.5)\%$. The reduction in MR ratio is due to the lead contact resistance [total lead plus sensor average resistance is (60 ± 10) Ω]. The average sensitivity is ~0.1%/Oe (corresponding to ~0.5 mV/Oe). The intrinsic sensitivity of the spin-valve sensors can be found from the ratio between the total resistance and the intrinsic resistance of the sensor: $\sim0.1\%/\text{Oe}\times60\ \Omega/46.2\ \Omega = 0.13\%/\text{Oe}$. The spin-valve sensors and leads were passivated with a 2000 Å thick sputtered SiO_2 layer for protection against the various fluids used during experimentation.

B. Tapered current lines

In addition to detection, one of our goals was to control the movement and placement of magnetically labeled biomolecules. To address this matter, on-chip tapered current line structures were designed and integrated with spin-valve sensors.[6] Each sensor had two adjacent Al current lines 10 μm apart (at the sensor site) with widths tapered from 150 μm at the contact pads to 5 μm at sensor sites. This provided a structure with increased current density at the desired locations adjacent to the sensor sites, resulting in higher local magnetic fields capable of attracting the labels to the sensor area. Using this technique, labels could be moved to and from the sensor surface and across it, either in few numbers[6] or in ensembles[7] [Figs. 2(a) and 2(b)]. In this way, labels were focused rapidly at sensor sites using currents of ~10–20 mA, considerably increasing the assay detection time.

Other workers have also reported the on-chip manipulation of magnetic particles using current line structures, either in conjunction with microfluidics for particle sorting[10] or for concentrating particles in particular regions using microcoils or current line matrixes.[11] Other current line architectures have been designed for single particle handling,[12] but their integration with a detection system such as this remains unique.

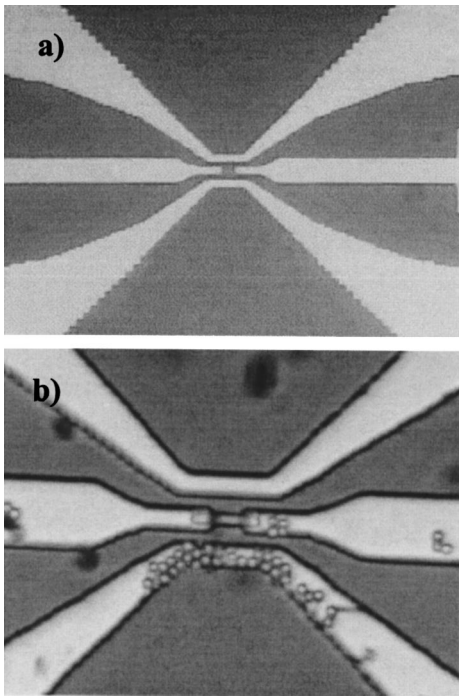

FIG. 2. (a) Design including a spin-valve sensor and adjacent tapered current lines for controlled placement and movement of the labels. (b) Current flows through the bottom current line attracting particles to the thinner region of the line.

C. Chip design

Different chip designs were developed for the detection or both the controlled placement and detection of magnetic labels. In the first stages of the work, an $8\times8\ mm^2$ chip featured six sensors ($2\times6\ \mu m^2$) each having two associated current lines for moving the labels (Fig. 2). First results on particle detection were obtained with this chip using single spin-valve sensors.[6] A second chip was designed exclusively for the detection of labels (Fig. 3). This chip was also $8\times8\ mm^2$ with 12 pairs of sensors, each pair having one sensor covered with photoresist [(PR) 1.5 μm] and the other sensor exposed ($25\times25\ \mu m^2$ sensing area) for the purpose of immobilizing biotin to the exposed SiO_2 area over the sensor. The two sensors in each pair, one used for binding detection (exposed) and the other used as reference (PR covered), were ~75 μm apart with a common input contact and two independent output contacts, enabling both single and differential sensor measurements. For differential measurements, a load resistor of ~0.5 kΩ was connected in series with each sensor of the pair to maintain a constant sense current through each sensor. Approximately 50 chips were fabricated per 3 in. Si wafer. The wafer was cut with a dicing saw and each chip was then mounted in a 40-pin side-brazed chip carrier. The contacts were made via wire bonding and were protected with a silicon gel (Elastosil E41).

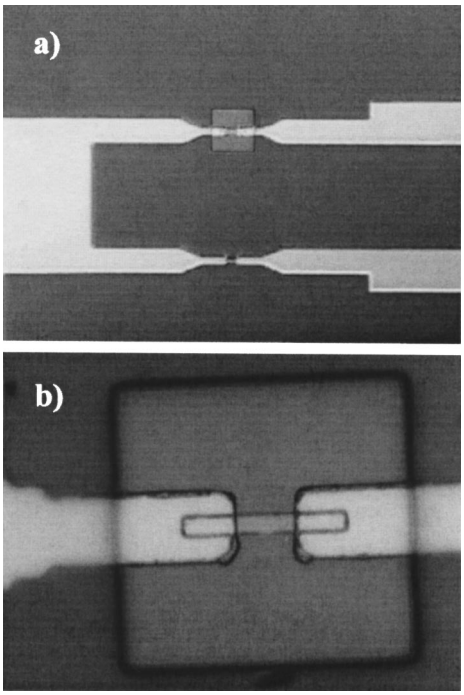

FIG. 3. (a) Design for differential measurements: one ''signal'' sensor with a $25\times25\ \mu m^2$ ''hole'' in photoresist and a ''reference'' sensor covered with photoresist. (b) Enlargement showing the $25\times25\ \mu m^2$ biotinylated SiO_2 surface on top of the signal sensor.

D. Experimental setup

The chip carrier was mounted in a small breadboard housed within an aluminum noise reduction box ($2\times6\times10\ cm^3$) fitted with a small hole in the top surface, corresponding to the position of the chip. The box could be then placed beneath an optical microscope so that the micron-sized labels could be observed during each experiment. Coaxial cables were used to make the electrical connections to the associated hardware, namely power sources and general purpose interface bus (GPIB)-controlled multimeters. A small (5 cm diameter) planar electromagnet with a $Ni_{80}Fe_{20}$ circular core was positioned over the top surface of the chip box, in order to apply an in-plane magnetic field (~15 Oe) in the sense direction of the sensors (transverse to the length of the sensors). This field was used to induce a moment within the superparamagnetic labels.

The experiments were performed using small volumes (5–10 μl) of fluid (water or *p*H of 7 buffer) with ~8 mA sense current per sensor, ~10–20 mA through the tapered current lines (when used), and an in-plane applied field of 15–18 Oe. The voltage drop across the sensor was measured directly using GPIB-controlled multimeters and the acquired data fed to a computer. Control experiments were performed using fluid samples without magnetic beads present to assess potential background signals arising from the addition of fluid to the chip, application of current to the current lines and other environmental changes.

E. Sensor surface functionalization

The SiO_2 surface over the exposed sensors was biotinylated using a standard procedure. The surface was treated with a 10% aqueous solution of 3-aminopropyltriethoxysilane for 20 min at room temperature, then washed with water followed by 100 mM phosphate buffer, *p*H of 7 and, finally, 100 mM phosphate buffer, *p*H of 7, containing 150 mM NaCl. The surface was then treated with a 0.75 mg/ml solution of sulfo-NHS-LC-biotin (Pierce) in the same phosphate buffered saline. After 40 min at room temperature, the cross linker was washed away with phosphate buffer and the streptavidin-functionalized labels introduced. In real-time signal data experiments, the sensors saturated with labels were only left for ~3 min before unbound labels were washed away.

TABLE I. Properties of the superparamagnetic labels used. The moment per particle is given for a 15 Oe magnetizing field and the magnetic susceptibility per particle is determined for an applied field range of ±50 Oe.

Particle type	Size (nm)	Iron oxide content (w/w)	Moment/particle (emu)	χ_m/particle (emu/Oe)
Micromer®-M	2000	15%	2×10^{-12}	1.3×10^{-13}
Nanomag®-D	250	75%–80%	2×10^{-13}	2.9×10^{-15}[a]
Nanomag®-D-spio	100	35%	2×10^{-16}	1.2×10^{-17}
Nanomag®-D-spio	50	35%	5×10^{-17}	3.7×10^{-18}

[a]For $10<|H|<50$ Oe.

F. Magnetic labels

The magnetic labels used in these systems are superparamagnetic, usually composed of iron oxide (magnetite) dispersed in a polymer matrix. These labels can be prepared with various surface functionalizations for binding to different types of biomolecules: Proteins, antibodies, or nucleic acids. In our work, 2 μm Micromer®-M microspheres, 250 nm Nanomag®-D, and 100 and 50 nm Nanomag®-D-spio particles obtained from Micromod GmbH, Germany were used (Table I). The smaller particles are irregularly shaped and have a tendency to cluster, whilst the microspheres are very uniform in size and shape allowing for quantification of number of labels detected. The magnetic moment per particle and the magnetic susceptibility per particle were determined by vibrating sample magnetometer measurements of liquid samples of known particle concentrations. These measure-

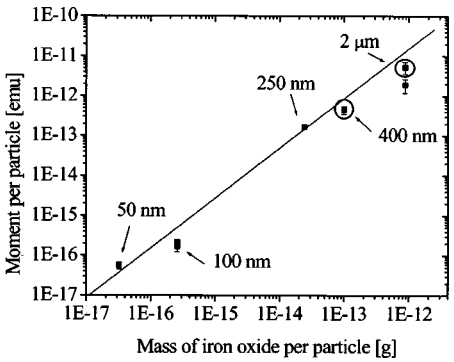

FIG. 4. Magnetic moment vs the mass of iron oxide for the magnetic labels studied. Circle-enclosed data correspond to data acquired previously for 2 μm Micromod®-M labels and for a developmental sample of 400 nm Nanomag®-D labels (as measured in Ref. 6).

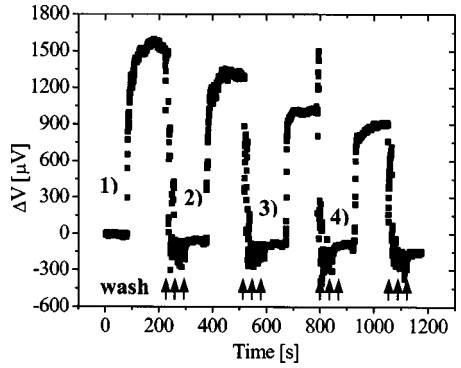

FIG. 5. Real-time data for saturation signals of various micron-sized magnetic labels: (1) 0.5–1.5 μm Magnabind™ (5 μl of ~15 mg/ml), (2) 1 μm Sera-Mag™ (5 μl of ~30 mg/ml), (3) 1 μm Estapor® (5 μl of ~30 mg/ml), and (4) 2 μm Micromer®-M (5μl of ~25 mg/ml). (8 mA sense current; 15 Oe applied field).

ments were made in a low-field range (±100 Oe). Using the data from the supplier on particle density and assuming a spherical shape, a linear relation (in log/log scale) between the iron oxide content and the magnetic moment per particle was observed (Fig. 4).

As a means of comparison, other micron-sized particles were also studied: 1 μm Estapor® from Indicia, 0.5–1.5 μm Magnabind™ from Pierce, and 1 μm Sera-Mag™ from Seradyn. The Magnabind™ beads were found to have a magnetic moment per particle of $\sim 9\times10^{-12}$ emu at 15 Oe and a magnetic susceptibility per particle of $\sim 5.94\times10^{-13}$ emu/Oe in the ±50 Oe range. Moment measurements for the other label products were not possible, as the necessary physical data were not available from the supplier.

III. RESULTS AND DISCUSSION

A. Detection of micron-sized magnetic labels

In our initial detection experiments[6,8] single detection of 2 μm Micromer®-M microspheres was achieved (~100–400 μV) with corresponding saturation signals of ~1 mV. Linearity between label number and signal was observed up to 6–10 labels over the sensor. For greater numbers of labels (>10), the signal variation was much reduced, as the labels were further from the sensor surface, contributing only with small fringe signals. More recently, the corresponding saturation signals for other commercially available micron-sized magnetic labels was studied (Fig. 5). Saturation signals of ~1 mV for the 2 μm Micromer®-M were confirmed, while for Magnabind™ a higher saturation signal (~1.6 mV) was obtained. This may be due to the higher magnetic moment per label (at 15 Oe) $\sim 9\times10^{-12}$ emu compared to 2×10^{-12} emu for the Micromer®-M and/or the difference in label size. Magnabind™ labels vary in size between 0.5–1.5 μm and may pack more efficiently over the sensor. This may also explain why the 1 μm sized labels Sera-Mag™ and Estapor® also gave higher saturation signals. However, when examined using light microscopy, the Micromer®-M labels seem by far the most uniform in size and shape and can be clearly quantifiable at the single-label level. For this reason, Micromer®-M labels were chosen for further work.

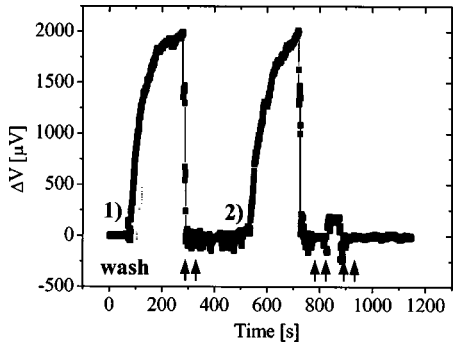

FIG. 6. Real-time data for saturation signals of 250 nm Nanomag®-D magnetic labels. (1) and (2) represent the introduction of 5 μl of 1 mg/ml solution ($\sim 3\times10^{10}$ particles/ml). (8 mA sense current; 18 Oe applied field).

B. Detection of nanometer-sized magnetic labels

Our present studies include the determination of detection signals for smaller magnetic labels. Figure 6 shows saturation signals for 250 nm Nanomag®-D particles functionalized with streptavidin. At high particle concentrations (3×10^{10} particles/ml), the signals were approximately 2 mV. This may be a consequence of a high iron-oxide content (75%–80%), compared with Micromer®-M labels (15%), resulting in a relatively high magnetic moment per particle volume. The magnetic moment per particle was determined to be 2×10^{-13} emu at 15 Oe (Table I). Comparing label size with sensor surface area, one layer of 250 nm labels may consist of >200 individual labels, while the same area can only accommodate three 2 μm labels.

The detection of smaller labels, 100 nm and 50 nm Nanomag®-D-spio is shown in Fig. 7 in comparison with the saturation signal for Magnabind™ labels. In this instance, very high label concentrations (10^{13}–10^{14} particles/ml) only give small saturation signals in the order of 600 or 300 μV, respectively. This would appear to be a consequence of their small moment per label (Table I). In order to produce a total moment of 2×10^{-12} emu (equivalent to one 2 μm label) about 10^4 100 nm labels would be required (having a moment per label of 2×10^{-16} emu) or $\sim 4\times10^4$ 50 nm labels (having a moment per label 5×10^{-17} emu). In practice, only

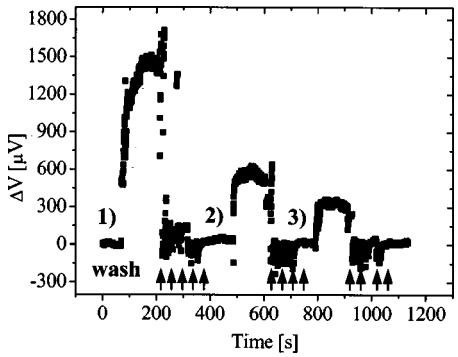

FIG. 7. Real-time data for saturation signal of (1) 0.5–1.5 μm Magnabind™ (5 μl of ~15 mg/ml, $\sim 7.5\times10^9$ particles/ml); (2) 100 nm Nanomag®-D-spio (5 μl of ~50 mg/ml; $\sim 7.5\times10^{13}$ particles/ml), and (3) 50 nm Nanomag®-D-spio (5 μl of ~50 mg/ml; $\sim 5.5\times10^{14}$ particles/ml) magnetic labels. (8 mA sense current; 15 Oe applied field).

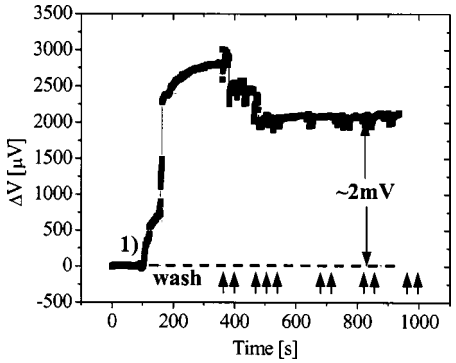

FIG. 8. Real-time data for binding detection of 250 nm Nanomag®-D streptavidin-functionalized magnetic labels to a biotinylated SiO_2 surface. (1) Addition of 5 μl of 2 mg/ml; $\sim 6\times10^{10}$ particles/ml. (8 mA sense current; 18 Oe applied field).

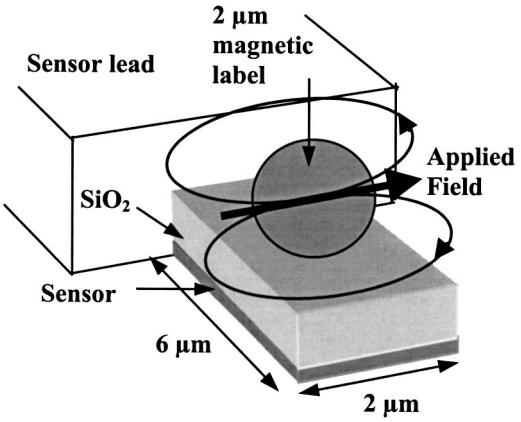

FIG. 9. Schematic of the detection of magnetic labels using spin-valve sensors.

~1200 (100 nm labels) or ~4800 (50 nm labels) can accumulate per layer over the sensor surface. In addition, the field contribution from each layer of labels decreases with increasing distance from the sensor.

C. Detection of biomolecular recognition

The detection of biomolecular recognition between biotin and streptavidin using 2 μm Micromer®-M labels[8] was previously demonstrated. Since then, the detection of biomolecular recognition using 250 nm labels using the same binding protocol was achieved. Figure 8 shows the detection signal profile for the addition of 250 nm labels, functionalized with streptavidin, to a biotinylated sensor surface. The sensor was first saturated with labels and then repeatedly washed with phosphate buffer. A residual signal of ~2 mV was obtained, in contrast to the same experiment performed with an untreated sensor, where the signal was observed to return to the base line immediately upon washing of the sensor (Fig. 6). As yet, the detection of biotin–streptavidin binding using smaller labels (<250 nm) was not achieved. Using the moment per label, it can be calculated that streptavidin-functionalized 100 nm labels would not give a sufficient residual binding signal, with the present setup. One layer of 100 nm labels (~1200) covering the sensor surface gives a total moment of $\sim 2\times10^{-13}$ emu with a maximum signal of 25 μV, which is presently within our experimental (sensor plus electronics) noise level.

D. Detection limits

A theoretical study was performed on the detection limits of the system used. This took into consideration the sensor characteristics and the experimental setup conditions. The intrinsic noise of the spin-valve sensor has two main components: The Johnson or thermal noise and the $1/f$ magnetic noise. Since the measurements were performed at low frequencies (~1 Hz), the $1/f$ noise is preponderant. For a single domain spin-valve sensor within the linear regime of the transfer curve, the minimum detectable field[13] $\Delta H_{\min}$ was calculated using Eq. (1):

$$(\Delta H_{\min})^2 \approx \left[\frac{R}{S}\right]^2 \int_{\Delta f}\left[\frac{\gamma_H}{N_c f}\right] df, \tag{1}$$

where R is the resistance value of the spin-valve sensor (~46.2 Ω); S is the intrinsic sensitivity of the sensor (0.06 Ω/Oe), γ_H is the Hooge's constant (~0.2 in the spin-valve linear regime), N_c is the number of charge carriers in the noisy volume, assuming one carrier per atom of the spin-valve sensor ($\sim 3\times10^{10}$), and Δf is the experimental frequency bandwidth (1 Hz).

The value for $\Delta H_{\min}$ was found to be in the order of 1.6 mOe, corresponding to an output change of 0.8 μV for a sense current of 8 mA. Using a simple magnetic model, where the magnetic label is placed at the center of the 2×6 μm^2 spin-valve sensor and applying a ~15 Oe in-plane magnetizing field along the easy axis of the sensor (perpendicular to the length of the sensor), the dipole field was calculated at the plane of the sensor. The distance between the sensor and the label is represented as the radius of the particle plus the thickness of the passivation layer (~2000 Å SiO_2). A schematic for this model is shown in Fig. 9. The space between the label and passivation layer occupied by the biomolecules used to immobilize the label on the surface (biotinylated cross linker plus streptavidin) and the distance between the sensor surface and the sensing layer were both considered negligible. The average of the field component along the sensing direction of the sensor (easy axis direction) was used in the determination of the overall resistance change of the sensor, although the total resistance change is smaller due to current redistribution within the sensor.[14] Using the magnetic moments of the labels shown in Table I, the expected sensor signals were calculated. For a spin-valve sensor with the characteristics described and with a bias current of 8 mA, the expected signals for one 2 μm Micromod®-M label (Fig. 10) and for one 250 nm Nanomag®-D particle were in the order of 100 μV and 25 μV, respectively. It was seen that the output signal is largely influenced by the sensitivity of the sensor and also by its resistance. This may explain the variation found in the individual signals recorded for single 2 μm labels (100–400 μV),[6,8] using different spin-valve sensors. Increased signals can also result from using a thinner passivation layer. Using

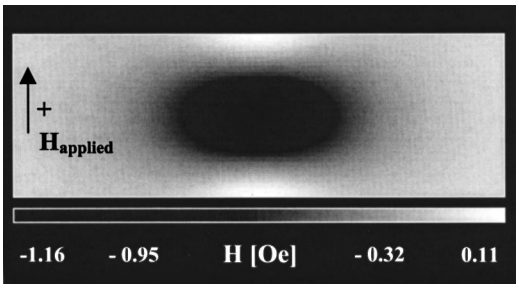

FIG. 10. Component of the magnetic field along the sensing direction of the sensor for a 2 μm Micromer®-M magnetic label calculated at the plane of the sensor. An external applied field ($H_{applied}$) in the sensing direction of the sensor is used to induce a moment in the superparamagnetic label.

the same reasoning, it was found that a superparamagnetic label with moment of $\sim 6\times 10^{-15}$ emu would generate a signal at the intrinsic noise level of the sensor (1.6 mOe average field; 0.8 μV change). Consequently, 100 and 50 nm labels with moments of 2×10^{-16} and 5×10^{-17} emu would not be detected at the single label level. Although the theoretical noise voltage change limit was calculated to be $\sim$0.8 μV, the experimental noise was shown to be in the order of 10–20 μV. This limits the measurable moments to the order of 2×10^{-13} emu, which corresponds to the detection of a single 250 nm label. Until now, detection of single 250 nm labels was not yet possible due to label clustering. This effect may be overcome to some extent via polymer encapsulation.

At present, the measured noise level can be reduced if other detection methods such as lock-in techniques are used. Also, the detection limit can be improved if the sensor is tailored to the magnetic label size.[14]

IV. CONCLUSIONS

Magnetic label detection signals and signal-to-noise ratios depend on the type of sensor used, sensor dimensions, label size and moment, experimental conditions, and amplification techniques. Various sensors have been investigated, large GMR sensors ($>80\times 5\ \mu m^2$),[2–5] spin-valves ($2\times 6\ \mu m^2$),[6–8] and Hall sensors ($2.4\times 2.4\ \mu m^2$),[9] each offering a particular advantage. The use of large GMR sensors allows for the detection of large numbers of magnetic labels, which may be advantageous for bioassays based on an increased number of biological interactions e.g., DNA screening. Spin valves offer increased sensitivity at the single-label detection level, which may exploitable in the detection of single biomolecular interactions and may lead to magnetic random access memorylike bioassays capable of screening thousands of different analytes. Finally, Hall sensors based on standard complementary metal–oxide–semiconductor technology offer easy integration with on on-chip electronics. In conclusion, the type of sensor used in a device may be tailored toward the chosen biological application.

Most of the work to date has focused on the detection of micron-sized labels, which may reflect the sensitivity of the systems used. While the initial use of micron-sized labels was essential for optical verification of label position over the sensor, their use in certain bioassays may reduce sensitivity due to masking of neighboring biomolecules by the large label. In the course of investigating smaller labels, we have demonstrated the detection of nanometer-sized labels between 250 and 50 nm. Present calculations, based on our present setup, indicate that single 250 nm labels can be detected and we are now developing sub-micron sized sensors for the detection of even smaller labels. Further developments for this promising field are foreseen with applications ranging from genomic research to drug development to diagnostics.

ACKNOWLEDGMENTS

The authors would like to thank the INESC engineers F. Silva, J. Bernardo, J. Faustino, and V. Soares for their technical assistance. Two of the authors (H. A. F. and D. L. G.) thank FCT for their doctoral SFRH/BD/5031/2001 and postdoctoral SFRH/BPD/3634/2000 grants, respectively. The Portuguese POCTI Biochip project, Contract No. 34459/99 and EU FP5 CF-Chip project, Contract No. QLK3-CT-2001-01982, supported this work.

[1] R. Shieh and D. E. Ackley. US Patent No 6,057,167 (May 2, 2000).
[2] D. R. Baselt, G. U. Lee, M. Natesan, S. W. Metzger, P. E. Sheehan, and R. J. Colton, Biosens. Bioelectron. **13**, 731 (1998).
[3] R. L. Edelstein, C. R. Tamanaha, P. E. Sheehan, M. M. Miller, D. R. Baselt, L. J. Whitman, and R. J. Colton, Biosens. Bioelectron. **14**, 805 (2000).
[4] M. M. Miller, P. E. Sheehan, R. L. Edelstein, C. R. Tamanaha, L. Zhong, S. Bounnak, L. J. Whitman, and R. J. Colton, J. Magn. Magn. Mater. **225**, 138 (2001).
[5] J. Schotter, P. Kamp, A. Becker, A. Puehler, D. Brinkmann, W. Schepper, H. Brueckl, and G. Reiss, IEEE Trans. Magn. **38**, 3365 (2002).
[6] D. L. Graham, H. Ferreira, J. Bernardo, P. P. Freitas, and J. M. S. Cabral, J. Appl. Phys. **91**, 7786 (2002).
[7] L. Lagae, R. Wirix-Speetjens, J. Das, D. Graham, H. Ferreira, P. P. Freitas, G. Borghs, and J. De Boeck, J. Appl. Phys. **91**, 7445 (2002).
[8] D. L. Graham, H. A. Ferreira, P. P. Freitas, and J. M. S. Cabral, Biosens. Bioelectron. (to be published).
[9] P. Besse, G. Boero, M. Demierre, V. Pott, and R. Popovic, Appl. Phys. Lett. **80**, 4199 (2002).
[10] M. Tondra, M. Granger, R. Fuerst, M. Porter, C. Nordman, J. Taylor, and S. Akou, IEEE Trans. Magn. **37**, 2621 (2001).
[11] C. S. Lee, H. Lee, and R. M. Westervelt, Appl. Phys. Lett. **79**, 3308 (2001).
[12] T. Deng, G. M. Whitesides, M. Radhakrishan, G. Zabow, and M. Prentiss, Appl. Phys. Lett. **78**, 1775 (2001).
[13] B. Raquet, *Spin Electronics* (Springer, Berlin, 2001), pp. 232–273.
[14] M. Tondra, M. Porter, and R. Lipert, J. Vac. Sci. Technol. A **18**, 1125 (2000).